

# Regeneration of pulp-dentine complex-like tissue in a rat experimental model under an inflammatory microenvironment using high phosphorous-containing bioactive glasses

J. Li , S. Wang  & Y. Dong 

Department of Cariology and Endodontology, Peking University School and Hospital of Stomatology, Beijing, China

## Abstract

**Li J, Wang S, Dong Y.** Regeneration of pulp-dentine complex-like tissue in a rat experimental model under an inflammatory microenvironment using high phosphorous-containing bioactive glasses. *International Endodontic Journal*, 54, 1129–1141, 2021.

**Aim** To investigate the effects of a bioactive glass with a high proportion of phosphorus (BG-hP) on the repair and regeneration of dental pulps in rats under an inflammatory microenvironment.

**Methodology** Human dental pulp cells (hDPCs) stimulated with  $1 \mu\text{g mL}^{-1}$  lipopolysaccharide (LPS) were co-cultured with  $0.1 \text{ mg mL}^{-1}$  BG-hP. Cell proliferation was detected by 3-[4,5-dimethylthiazol-2-yl]-2,5 diphenyltetrazolium bromide (MTT) assays. The expression of inflammation-related genes and odontogenic differentiation-related genes was determined by real-time PCR. Alizarin red staining was used to detect the formation of mineralized nodules. Coronal pulp tissues of rat molars were stimulated with  $10 \text{ mg mL}^{-1}$  LPS and then treated with BG-hP. The expression of inflammation-related genes in pulp tissue was determined by real-time PCR. Haematoxylin-eosin staining and Masson staining were performed to observe the inflammatory response and mineralized matrix formation, after subcutaneous implantation in nude mice, at 3 days and 4 weeks, respectively. Analysis of variance was performed to measure statistical significance ( $P < 0.05$ ).

**Results** BG-hP significantly reduced expression of interleukin-6 (*IL-6*) and *IL-8* and significantly

upregulated the expression of *IL-10*, *IL-4* and transforming growth factor- $\beta 1$  of the LPS-stimulated hDPCs ( $P < 0.05$ ). BG-hP significantly inhibited the initial cell number ( $P < 0.05$ ), but the hDPCs stimulated by LPS and co-cultured with BG-hP maintained the same proliferation rate as the untreated hDPCs. BG-hP significantly promoted the expression of dentine matrix protein-1 and dentine sialophosphoprotein and the mineralization capacity of the LPS-stimulated hDPCs ( $P < 0.05$ ). Furthermore, BG-hP significantly downregulated the expression of *IL-6* and reduced the inflammatory response of the LPS-stimulated pulp tissue 3 days after subcutaneous implantation ( $P < 0.05$ ). Four weeks after subcutaneous implantation, BG-hP induced the formation of a continuous layer of dentine-like structure with dentinal tubules and polarizing odontoblast-like cells aligned along it in the LPS-stimulated pulp tissue.

**Conclusion** The present preliminary results demonstrated that the bioactive glass with a high proportion of phosphorus inhibited the inflammatory response and promoted the formation of a pulp-dentine complex in a rat experimental model. This study provides a foundation for the construction of materials with the dual functions of exerting anti-inflammatory effects and promoting tissue regeneration to meet the needs of dental pulp repair and regeneration.

**Keywords:** anti-inflammation, bioactive glass, dentine formation, lipopolysaccharide, pulp repair.

Received 7 May 2020; accepted 1 March 2021

Correspondence: Sainan Wang, Department of Cariology and Endodontology, Peking University School and Hospital of Stomatology, 22 Zhongguancun South Avenue, Beijing, 100081, China (e-mail: bdkqwsn@bjmu.edu.cn).

## INTRODUCTION

The biological aim of regenerative endodontic treatment is to maintain the structure of the pulp-dentine complex and its physiological function when the pulp is subjected to microbial infection. The appropriate regulation of inflammation is prerequisite for tissue repair and regeneration. Biomaterials may affect the inflammation response by modulating the release of pro- or anti-inflammatory cytokines by mesenchymal stem cells and macrophages (Sadowska *et al.* 2019). Clinically, the most commonly used bioactive materials in endodontic therapy are calcium silicate-based cements, such as MTA (Dentsply Tulsa, Johnson City, TN, USA), Biodentine (Septodont, St Maur des Fosses, France) and iRoot (Innovative BioCeramix Inc, Vancouver, BC, Canada). Although these materials have been reported to have good biocompatibility and sealing abilities and can induce the formation of dentine bridges, they are non-degradable (Bogen *et al.* 2008, Parirokh *et al.* 2018, Solanki *et al.* 2018, Torabinejad *et al.* 2018). Several studies have confirmed the anti-inflammatory capacity of these calcium silicate-based cements, but their anti-inflammatory effects remain controversial in general (Barbosa *et al.* 2008, Lee *et al.* 2019, Erakovic *et al.* 2020).

For regeneration of the pulp-dentine complex, biodegradable scaffolds are required and the materials should eventually be replaced by the regenerated tissues. Bioactive glasses (BGs) are biodegradable calcium silicate-based materials with a proven osteoinductive ability and are safe for use in the human body (Hench & Paschall 1973, Marrazzo *et al.* 2016). A previous study demonstrated that BGs could induce the odontogenic differentiation of dental pulp cells *in vitro* and promote pulp-dentine complex regeneration *in vivo* (Wang *et al.* 2014, Cui *et al.* 2017). On the other hand, recent studies have shown that BGs such as strontium-substituted bio-glass, 75S mesoporous BG and 45S5 BG inhibited inflammation and promoted healing in bone tissue and skin wounds (Jebahi *et al.* 2013, Gomez-Cerezo *et al.* 2018, Huang *et al.* 2018). Dong *et al.* (2017) reported that 45S5 BG regulated macrophage phenotypes and the extracellular matrix microenvironment in a paracrine manner and reduced the inflammatory response. The effects of BG on the inflammation regulation of dental pulps are worth further study.

Upon contact with water-rich human tissues, most BGs are associated with a significant local increase in

pH due to a rapid release of calcium and/or sodium ions (Gough *et al.* 2004, Midha *et al.* 2013). The extreme alkalinity may cause cell necrosis and apoptosis, possibly aggravating the inflammation response and pulp damage (Gandolfi *et al.* 2014, Hirose *et al.* 2016). In principle, increasing the phosphorus content of a BG could reduce the pH increase by combining the dissolved P with Ca to form precipitates (Donnell *et al.* 2008, Abou Neel *et al.* 2009). However, the phosphorus contents in traditional BGs, such as 45S5, 58S (58 wt% SiO<sub>2</sub>, 33 wt% CaO and 9 wt% P<sub>2</sub>O<sub>5</sub>) and 77S (58 wt % SiO<sub>2</sub>, 33 wt % CaO and 9 wt % P<sub>2</sub>O<sub>5</sub>), are below 10 wt % due to the limitations of their method of preparation (Silver *et al.* 2001). In the melt-quenching method, increasing phosphorus can inhibit the glass-forming ability, while in conventional sol-gel methods, the hydrolysis of alkyl phosphates is slow and phosphate precipitation tends to occur instead of gelation (Abou Neel *et al.* 2009). Recently, a novel BG was synthesised using non-toxic phytic acids as the phosphorus precursors, which could achieve much higher phosphorus concentrations (22.7 wt % P<sub>2</sub>O<sub>5</sub>, 48.2 wt % SiO<sub>2</sub> and 29.1 wt % CaO) compared to traditional BG without affecting the network connectivity/dissolution, thus helping stabilize neutral conditions (Li & Qiu 2011). A previous study has demonstrated that this novel BG with a high proportion of phosphorus significantly promoted the odontogenic differentiation of dental pulp cells and induced more typical dentine-like tissues with odontoblast-like cells generated compared with traditional BG 45S5 (Cui *et al.* 2017).

In this study, the effects of this BG with a high proportion of phosphorus (abbreviated as BG-hP in this study) on the repair and regeneration of dental pulp under a lipopolysaccharide (LPS)-stimulated inflammatory microenvironment were investigated.

## MATERIALS AND METHODS

### Cell culture

Extracted intact third molars were obtained from 18- to 25-year-old patients at the Oral Surgery Department of Peking University School and Hospital of Stomatology with informed consent and the approval of the ethics committee (PKUSSRB-202053006). Primary human dental pulp cells (hDPCs) were isolated according to the procedure reported by Gronthos *et al.* (2000). The hDPCs obtained were cultured in

Dulbecco's modified Eagle's medium (DMEM; Gibco BRL, Gaithersburg, MD, USA) containing 10% foetal bovine serum (FBS; Kangyuan, Tianjin, China) and 1% penicillin and streptomycin (Gibco) at 37 °C in 5% CO<sub>2</sub>. HDPCs were passaged at a ratio of 1 : 3 upon reaching 80% confluence. The medium was changed every 2 days. Cells between 4 and 6 passages were used for all experiments.

### HDPCs cultured with BG-hP and LPS

BG-hP with a composition of 22.7 wt % P<sub>2</sub>O<sub>5</sub>, 48.2 wt % SiO<sub>2</sub> and 29.1 wt % CaO was prepared by the sol-gel method using phytic acid (Sigma-Aldrich, St. Louis, MO, USA) as the precursor of phosphorus (Li & Qiu 2011). In brief, phytic acid and ethanol were mixed with water at room temperature, tetraethyl orthosilicate (Sinopharm Chemical Reagent Co Ltd, Shanghai, China) was added under magnetic agitation for 1 h, and then, Ca(NO<sub>3</sub>)<sub>2</sub>·4H<sub>2</sub>O powder (Sinopharm Chemical Reagent Co Ltd) was added to form a transparent sol, which was gelatinized at room temperature in a polypropylene container. After ageing at 60 °C for 1 week and then at 120 °C for another 2 weeks, the dry gel was ground into fine powder and sintered at a temperature of 300–400 °C to obtain BG-hP powder. After sterilization at 180 °C for 3 h, the BG-hP powder was mixed with anhydrous ethanol to form a BG-hP suspension at 0.1 mg mL<sup>-1</sup>. Then, 100 and 2972 µL of the BG-hP suspension per well were added into 96-well and 6-well culture plates (Costar; Corning, NY, USA), respectively, to produce an equivalent coating of BG-hP. The plates were air-dried in a laminar airflow cabinet to produce a stable adherent layer of BG-hP particles. HDPCs were then seeded onto BG-hP-coated plates and cultured in DMEM containing 1 µg mL<sup>-1</sup> LPS (*Escherichia coli*, Sigma-Aldrich) for 24 h, and afterward, the culture media were replaced with regular DMEM, as the LPS + BG-hP group. Cells seeded onto plates without the BG-hP coating were stimulated with LPS for 24 h as the LPS group, and cells without BG-hP and LPS stimulation served as the control group.

### Cell proliferation of hDPCs by MTT assays

HDPCs (5 × 10<sup>3</sup> cells per well) were seeded onto 96-well plates with or without LPS and BG-hP. The culture medium was changed every other day. After 1, 3, 5, and 7 days of culture, 180 µL of fresh DMEM and 20 µL of 5 mg mL<sup>-1</sup> 3-[4,5-dimethylthiazol-2-

yl]-2,5 diphenyltetrazolium bromide (MTT; Amresco, Solon, OH, USA) solution were added to each well and incubated for 4 h. Then, 150 µL of DMSO was added to each well and shaken for 10 min at 37 °C until the crystals at the bottom of the well were fully dissolved. The optical density (OD) was measured at 490 nm using a microtiter plate reader (BioTek, ELX808, Winooski, VT, USA). The live cell percentage was normalized with that of cells in the control group on day 1. The experiment was repeated independently three times.

### Gene expression of hDPCs by real-time reverse transcription–polymerase chain reaction (real-time PCR)

HDPCs (5 × 10<sup>5</sup> cells per well) were seeded onto 6-well plates with or without LPS and BG-hP. After 6, 24 h, 4 and 7 days of culture, the total cellular RNA of the three groups was obtained by adding TRIzol reagent (Invitrogen, Carlsbad, CA, USA) to the cell samples and then reverse-transcribed using PrimeScript<sup>TM</sup> RT Master Mix (Perfect Real Time; TaKaRa, Bio, Otsu, Japan). Real-time PCR was performed using the SYBR Premix Ex Taq<sup>TM</sup> Kit (TaKaRa) and the ABI QuantStudio 3 Real-Time PCR system. The primers for dentine sialophosphoprotein (*DSPP*), dentine matrix protein 1 (*DMP-1*), runt-related transcription factor 2 (*RUNX2*), osteocalcin (*OCN*), interleukin-4 (*IL-4*), *IL-6*, *IL-10*, transforming growth factor-β1 (*TGF-β1*), tumour necrosis factor-α (*TNF-α*) and glyceraldehyde-3-phosphate dehydrogenase (*GAPDH*) are listed in Table 1. The reaction system was 40 cycles at 95 °C for 15 s and at 60 °C for 60 s, followed by the thermal dissociation protocol for SYBR Green detection. The results were calculated from three independent experiments.

### Alizarin red staining of the mineralization of hDPCs

Cells were seeded onto 6-well plates at a density of 5 × 10<sup>5</sup> cells per well and cultured to reach 75–85% confluence, and then, the medium was changed to osteogenic-induced medium (OM) containing 2.16 mg mL<sup>-1</sup> β-glycerophosphate (Sigma-Aldrich), 100 µg mL<sup>-1</sup> L-ascorbic acid (Sigma-Aldrich) and 3.92 ng mL<sup>-1</sup> dexamethasone (Sigma-Aldrich). After 2 and 4 weeks of culture, the cells were fixed with 4% paraformaldehyde, stained with 40 mmol L<sup>-1</sup> alizarin red dye (pH 4.2) at room temperature for 20 min and

**Table 1** PCR primer sequences

Gene	Sequence (5'-3')
<i>DMP-1</i>	Forward: AGGAAGTCTCGCATCTCAGAG Reverse: TGGAGTTGCTGTTTTCTGTAGAG
<i>DSPP</i>	Forward: ATATTGAGGGCTGGAATGGGGA Reverse: TTTGTGGCTCCAGCATTGTCA
<i>IL-4</i>	Forward: CGGCAACTTTGTCCACGGA Reverse: TCTGTTACGGTCAACTCGGTG
<i>IL-6</i>	Forward: CCACTCACCTCTTCAGAACG Reverse: CATCTTTGGAAGGTTTCAGGTTG
<i>IL-8</i>	Forward: TTTTGCCAAGGAGTGCTAAAGA Reverse: AACCCCTCTGCACCCAGTTTTT
<i>IL-10</i>	Forward: GACTTTAAGGGTTACCTGGGTTG Reverse: TCACATGCGCCTTGATGTCTG
<i>GAPDH</i>	Forward: GAAGGTGAAGGTCGGAGTC Reverse: GAGATGGTGATGGGATTTT
<i>OCN</i>	Forward: AGGGCAGCGAGGTAGTGA Reverse: CCTGAAAGCCGATGTGGT
<i>RUNX2</i>	Forward: ACCCAGAAGGCACAGACAGAAG Reverse: AGGAATGCGCCCTAAATCACT
<i>TGF-<math>\beta</math>1</i>	Forward: CTAATGGTGGAAACCCACAACG Reverse: TATCGCCAGGAATTGTTGCTG
<i>TNF-<math>\alpha</math></i>	Forward: CCTCTCTCTAATCAGCCCTCTG Reverse: GAGGACCTGGGAGTAGATGAG
<i>Il-6</i>	Forward: TAGTCCTTCTACCCCAATTTCC Reverse: TTGGTCCTTAGCCACTCCTTC
<i>Gapdh</i>	Forward: GAAGGTGAAGGTCGGAGTC Reverse: GAGATGGTGATGGGATTTT
<i>Tnf-<math>\alpha</math></i>	Forward: TGTAGACCATGTAGTTGAGGTCA Reverse: GCTACGACGTGGGCTACAG

then rinsed with deionized water three times. The mineralized nodules were observed and photographed under an inverted microscope (Olympus, Tokyo, Japan). Alizarin red from the mineralized nodules was dissolved in 10% cetylpyridinium chloride (Sigma-Aldrich) for 30 min at room temperature. The OD was measured at 562 nm using a microliter plate reader. The cells cultured in DMEM served as the control in these experiments. The calcium concentrations were determined according to the absorbance at 562 nm using a standard calcium curve prepared in the same solution. The final calcium levels in each group were normalized to the total protein concentrations obtained from the duplicate plates.

### Gene expression of pulp tissues by real-time PCR

All animal experiments were conducted according to the accepted standards of humane animal care and approved by the Animal Care Committee of Peking University (LA2019358). Four-week-old Sprague-Dawley rats were anaesthetized and euthanized. The crowns of the fresh first molars, including the hard

tissue and coronal pulp tissue, were obtained by separation at the cemento-enamel junction using surgical blades. The crowns with coronal pulp were immersed in DMEM containing 10 mg mL<sup>-1</sup> LPS for 1 min to obtain the LPS-stimulated pulp tissues. The LPS-stimulated pulp tissues placed in BG-hP-coated plates containing DMEM comprised the LPS + BG-hP group ( $n = 6$ ). The LPS-stimulated pulp placed in plates without a BG-hP coating comprised the LPS group ( $n = 6$ ), while the pulp without LPS stimulation placed in plates without a BG-hP coating comprised the control group ( $n = 6$ ). After 3 h of incubation at 37 °C in 5% CO<sub>2</sub>, the pulp tissues in different groups were homogenized by a TissueLyser II (Qiagen, Germantown, MD, USA). The expression of inflammation-related genes (*Tnf- $\alpha$*  and *Il-6*) was determined by real-time PCR as previously described. The primer sets used to detect *Il-6*, *Gapdh* and *Tnf- $\alpha$*  are listed in Table 1.

### Subcutaneous transplantation of pulp tissues in nude mice

First, 10 mg of the disinfected BG-hP powders were mixed with 25  $\mu$ L DMEM to prepare a paste to cover the cross-section of LPS-stimulated pulp tissues (LPS + BG-hP group,  $n = 6$ ). The LPS-stimulated pulp tissues without BG-hP were served as the LPS group ( $n = 6$ ), and pulp tissues alone were served as the control group ( $n = 6$ ). After intraperitoneal injection of 30 mg kg<sup>-1</sup> of 0.5% pentobarbital sodium, the skin on the back of nude mice was disinfected with alcohol, a 5 mm incision was made in the skin on both sides of the back, and the subcutaneous tissue was blunt-separated to form a pouch (approximately 5  $\times$  10 mm). The crowns of the samples were gently implanted deep into the pouches, avoid touching the paste (Fig. 1). After 3 days and 4 weeks of subcutaneous implantation, the samples were retrieved, fixed in 4% polyoxymethylene, decalcified and then processed for haematoxylin-eosin (H&E) staining and Masson's trichrome staining (Baso Diagnostic Inc, Zhuhai, Guangdong, China) according to the manufacturer's recommended protocol.

### Statistical analysis

Statistical analyses were performed using SPSS (SPSS version 24.0; SPSS Inc, IBM, NY, USA). The results were analysed statistically by one-way analysis of variance (ANOVA) and Bonferroni's test (multiple

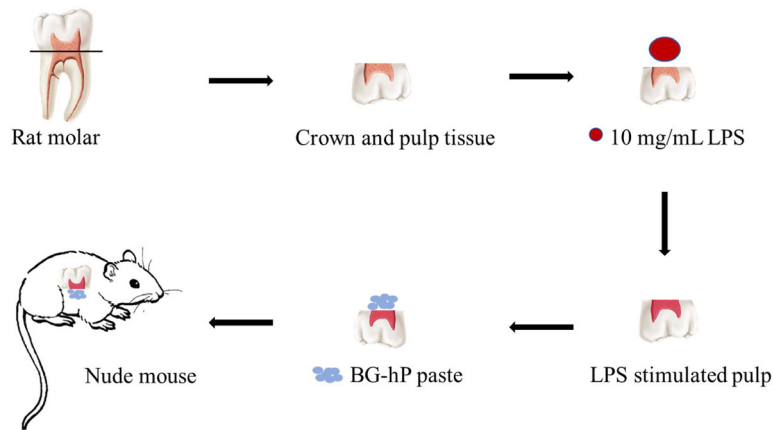


**Figure 1** Schematic diagram of subcutaneous transplantation in nude mice *in vivo*.

comparisons). If the data variance was uneven, the Kruskal-Wallis H-test was adopted, and  $P < 0.05$  was considered significant. Results are presented as mean  $\pm$  standard error of mean.

## RESULTS

### Effects of BG-hP on inflammation-related gene expression, proliferation, odontogenic differentiation and mineralization of hDPCs stimulated by LPS

Real-time PCR was used to detect the expression of inflammation-related genes in the hDPCs stimulated by LPS (Fig. 2a). After 6 h of co-culture of hDPCs and LPS, the expression of *TNF- $\alpha$*  ( $P = 0.001$ ), *IL-6* ( $P < 0.001$ ) and *IL-8* ( $P < 0.001$ ) was increased significantly in the LPS group compared with the control group. The expression of *IL-6* ( $P = 0.208$ ) and *TNF- $\alpha$*  ( $P = 0.352$ ) in the LPS + BG-hP group was not lower than in the LPS group, and the expression of *IL-8* was significantly decreased in the LPS + BG-hP group compared with the LPS group ( $P < 0.001$ ). After 24 h of co-culture of hDPCs and LPS, the expression of *IL-10* ( $P = 0.829$ ) and *IL-4* ( $P = 0.871$ ) was not lower than in the control group, and the expression of *TGF- $\beta$ 1* was decreased significantly in the LPS group compared with the control group ( $P < 0.001$ ). The expression of *IL-6* was significantly inhibited ( $P < 0.001$ ), and the expression of *IL-10* ( $P = 0.017$ ), *IL-4* ( $P < 0.001$ ) and *TGF- $\beta$ 1* ( $P = 0.0239$ ) was significantly upregulated in the LPS + BG-hP group compared with the LPS group.

The effect of BG-hP on the proliferation of hDPCs stimulated by LPS was detected by MTT assays (Fig. 2b). The relative amount of living cells in the LPS + BG-hP group was significantly lower than that in the control group ( $P < 0.001$  on days 1, 3, 5, 7, 9), while there was no significant difference between the control group and the LPS group ( $P = 1$ ). However, the relative proliferation rate in the LPS + BG-hP group, indicated by the slope of the growth curve, remained the same as that in the control group and the LPS group. The results suggested that BG-hP inhibited the initial cell number but had no effect on the cell proliferation rate of the LPS-stimulated hDPCs.

The expression of the odontogenic differentiation-related genes *RUNX2*, *OCN*, *DMP-1* and *DSPP* in the hDPCs stimulated by LPS was detected by real-time PCR (Fig. 2c). The results showed that *DMP-1* ( $P < 0.001$ ,  $< 0.002$  on days 4 and 7) and *DSPP* ( $P = 0.042$ ,  $0.0283$  on days 4 and 7) expression in the LPS + BG-hP group on days 4 and 7 was significantly higher than that in the control group and the LPS groups. There were no significant differences in the expression of *DMP-1* on days 4 ( $P = 1$ ) and 7 ( $P = 1$ ) or *DSPP* on day 4 ( $P = 0.438$ ) between the LPS group and the control group, while the expression of *DSPP* on day 7 in the LPS group was significantly higher than that in the control group ( $P = 0.0385$ ). There were no significant differences in the expression of *RUNX2* and *OCN* on day 4 among the three groups ( $P = 1$ ).

Alizarin red staining was used to detect the mineralization of hDPCs stimulated by LPS after 2 and

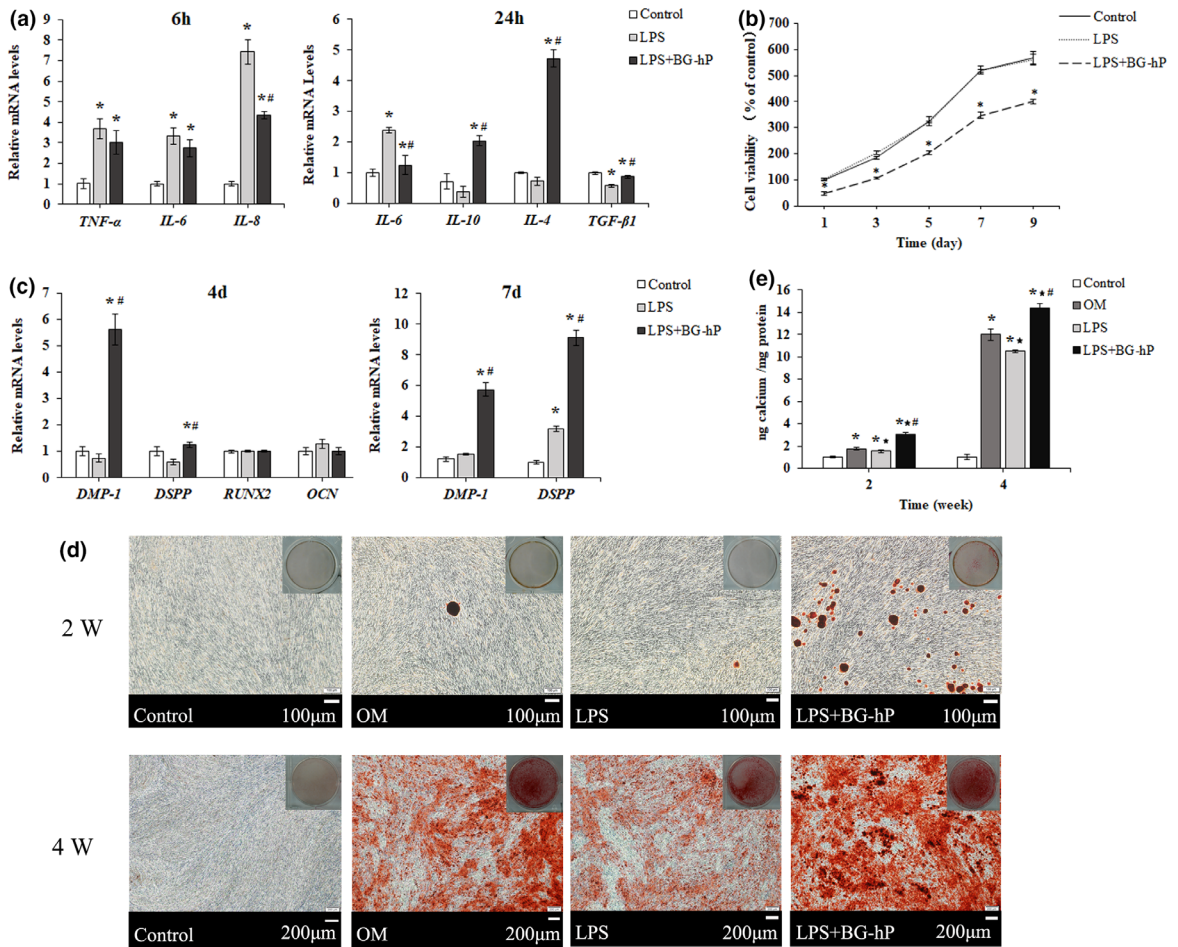


**Figure 2** Effects of BG-hP on inflammation-related gene expression, proliferation, odontogenic differentiation and mineralization of hDPCs stimulated by LPS. (a) Real-time PCR results of inflammation-related gene expression at 6 and 24 h; (b) Growth curves detected by MTT assays; (c) Real-time PCR results of odontogenic differentiation genes; (d) Alizarin red staining of mineralized nodules; and (e) Calcium concentration in (c) by cetylpyridinium chloride detection. Each value represents the mean ± SD ( $n = 3$ ). \* $P < 0.05$ , versus the corresponding control group; # $P < 0.05$ , versus the corresponding LPS group; \* $P < 0.05$ , versus the corresponding OM group.

4 weeks of osteogenic induction culture (Fig. 2d). At 2 weeks, a few red-stained mature mineralized nodules were formed in the LPS + BG-hP group, while single mineralized nodules were found in the OM group and the LPS group. At 4 weeks, many mature, red-stained mineralized nodules were observed in the LPS + BG-hP group, many more than those in the OM group and the LPS group. No mineralized nodules were found in the control group at 2 and 4 weeks. According to semi-quantitative detection of the mineralized nodules by dissolution in cetylpyridinium chloride (Fig. 2e), the calcium content of the LPS + BG-hP group was significantly higher than that of the

OM group ( $P = 0.017$ ,  $<0.001$  at 2 and 4 weeks) and the LPS group ( $P = <0.001$  at 2 and 4 weeks, respectively). LPS inhibited significantly the mineralization of hDPCs, while BG-hP promoted significantly the mineralization of the LPS-stimulated hDPCs.

### Effects of BG-hP on the inflammatory response and the formation of the pulp-dentine complex of pulp tissues stimulated by LPS

The expression of *Il-6* and *Tnf-α* in pulp tissue was detected after 3 h of co-culture of the LPS-stimulated

pulp tissue and BG-hP (Fig. 3a). The expression of *Il-6* ( $P = 0.0152$ ) and *Tnf- $\alpha$*  ( $P = <0.001$ ) in the LPS group was significantly higher than that in the control group. The expression of *Il-6* in the LPS + BG-hP group was significantly lower than that in the LPS group ( $P = <0.001$ ), and the expression of *Tnf- $\alpha$*  was not lower than that in the LPS group ( $P = 0.341$ ).

After 3 days of subcutaneous implantation in nude mice, HE staining was performed to observe the effects of BG-hP on the inflammatory response of the LPS-stimulated pulp tissue. The pulp in the control group had normal morphology without any inflammatory response. The predentine and odontoblastic layers were basically intact, and no inflammatory cells were

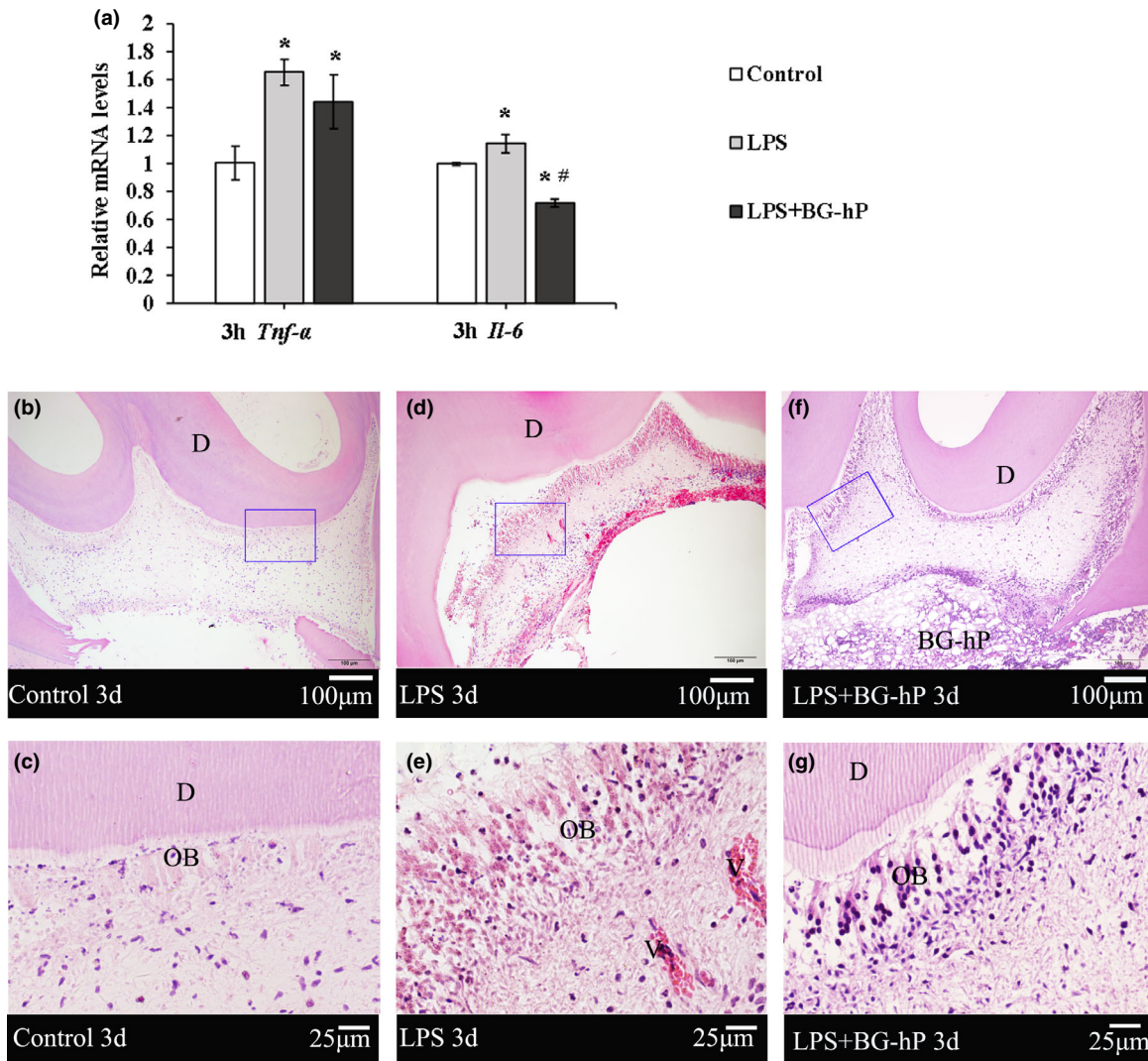


**Figure 3** Effects of BG-hP on the inflammatory response of pulp tissue stimulated by LPS. (a) Real-time PCR results of inflammation-related gene expression in LPS-stimulated pulp tissue treated with or without BG-hP at 3 h. HE staining (b–g) of crowns 3 days after subcutaneous transplantation in nude mice *in vivo*. (b,c) Crowns transplanted alone (c is a magnified image of the blue-boxed areas in b); (d,e) Crowns pretreated with 10 mg mL<sup>-1</sup> LPS (e is a magnified image of the blue-boxed areas in d); (f,g) Crowns pretreated with 10 mg mL<sup>-1</sup> LPS and covered with BG-hP (g is a magnified image of the blue-boxed areas in f). Each value represents the mean  $\pm$  SD ( $n = 3$ ). \* $P < 0.05$  versus the corresponding control group; # $P < 0.05$  versus the corresponding LPS group. Abbreviations: D, dentine; OB, odontoblast; V, blood vessel.

observed in the pulp tissue (Fig. 3b,c). The pulp in the LPS group had a moderate inflammatory response. Inflammatory cells and dilated blood vessels were observed in the pulp tissue. The predentine and odontoblastic layers were broken (Fig. 3d,e). The pulp in the LPS + BG-hP group had a mild inflammatory response. There was little inflammatory cell infiltration, while the predentine and odontoblastic layers were basically intact (Fig. 3f,g).

After 4 weeks of subcutaneous implantation in the nude mice, HE staining and Masson trichrome staining were performed to observe the effects of BG-hP on pulp-dentine complex formation in the LPS-stimulated pulp tissue. In the control group, the pulp tissue was normal without an inflammatory response. The vascular structure was observed, and matrix was formed below the primary dentine of the crown (Fig. 4a,b). Many collagen fibres were observed on the cross-section of the pulp in the LPS group. Sporadic osteodentine-like matrix areas were generated in the pulp (Fig. 4c,d). In the LPS + BG-hP group, BG-hP particles were surrounded by fibrous tissue. A layer of newly generated matrix with typical dentinal tubule structure was observed in the pulp-BG-hP interface, and polarizing columnar cells were found aligned along this matrix. The pulp tissue appeared normal and contained many blood vessels. A newly generated matrix was also observed below the primary dentine of the crown (Fig. 4e,f). Masson trichrome staining revealed many blue-dyed collagen fibres without mineralization in the pulp of the control group (Fig. 4g, h). In the LPS group, a few blue-stained irregular mineralized matrices with scattered cells embedded inside were generated in the pulp tissue, and blue-dyed collagen fibres without obvious mineralization were observed in the pulp cross-section (Fig. 4i,j). In the LPS + BG-hP group, blue-stained mineralized matrix with dentinal tubules was observed around the BG-hP particles and was integrated into an intact layer in the pulp-BG-hP interface (Fig. 4k,l).

## DISCUSSION

Lipopolysaccharide is commonly used to stimulate dental pulp cells to mimic the inflammatory microenvironment *in vitro* and to establish a pulpitis model *in vivo* (Renard *et al.* 2016, Bindal *et al.* 2018). The increase in TNF- $\alpha$ , IL-6 and IL-8 in hDPCs stimulated by LPS indicated the presence of inflammation in this study. Subcutaneous transplantation of the composite of material and pulp in nude mice was used to

directly observe the effect of BG-hP on dental pulp tissue (Wang *et al.* 2014) and verified inflammatory response in LPS-stimulated pulp *in vivo*.

In this study, BG-hP promoted the expression of cytokines IL-10, IL-4 and TGF- $\beta$ 1 and inhibited the expression of cytokines IL-6 and IL-8 in the LPS-stimulated dental pulp. The immunomodulatory activity of mesenchymal stem cells in pulp tissue is the key in the regulation of pulp inflammation and dental tissue-derived stem cells have been reported to possess immunosuppressing properties (Li *et al.* 2014, Ballini *et al.* 2017, 2018). The types and expression levels of inflammatory-related cytokines affect the progression and outcome of pulp inflammation (Farges *et al.* 2011). Several studies have reported that the concentrations of IL-6 and IL-8 are significantly higher in inflamed dental pulps than in healthy pulps (Barkhordar *et al.* 1999, Zehnder *et al.* 2003, Elsalhy *et al.* 2013), indicating their pro-inflammatory role. IL-6 has generally been considered as a pro-inflammatory marker within 24 h in LPS-treated hDPCs or pulp tissues (Renard *et al.* 2016, Jung *et al.* 2017, Sugiuchi *et al.* 2018, Zhu *et al.* 2019). However, IL-6 also act as an anti-inflammatory cytokine, such as in the co-culture system of hDPCs and peripheral-blood mononuclear cells at 72 h (Hossein-Khannazer *et al.* 2019), suggesting that the effect of IL-6 may be related to the microenvironment and its expression time. In contrast, some cytokines, such as IL-10 and IL-4, inhibit excessive inflammatory responses and promote repair (Tokuda *et al.* 2002, Cao *et al.* 2014, Shao *et al.* 2020). TGF- $\beta$ 1, as an anti-inflammatory cytokine, could activate M2 macrophages and promote the odontogenic differentiation of dental pulp cells (Martinez *et al.* 2008, Park *et al.* 2017). IL-10 produced by DPSCs could reduce pro-inflammatory cytokines and increase M2 macrophages (Omi *et al.* 2016). The present study reported that BG-hP alleviated the inflammatory response of dental pulp tissue under LPS stimulation by decreasing the expression of pro-inflammatory cytokines and promoting the expression of anti-inflammatory cytokines.

The ability of BG-hP to inhibit the inflammatory response of pulp tissue may be related to its release of calcium and silicon ions from biomaterials. Silicon and calcium ions released from calcium phosphate bioceramics regulate host immunity and promote macrophage apoptosis in a concentration-dependent manner by inhibiting LPS-activated MAPK and NF- $\kappa$ B pathways (Huang *et al.* 2018). Elevated calcium ions in the extracellular matrix inhibit the NF- $\kappa$ B pathway

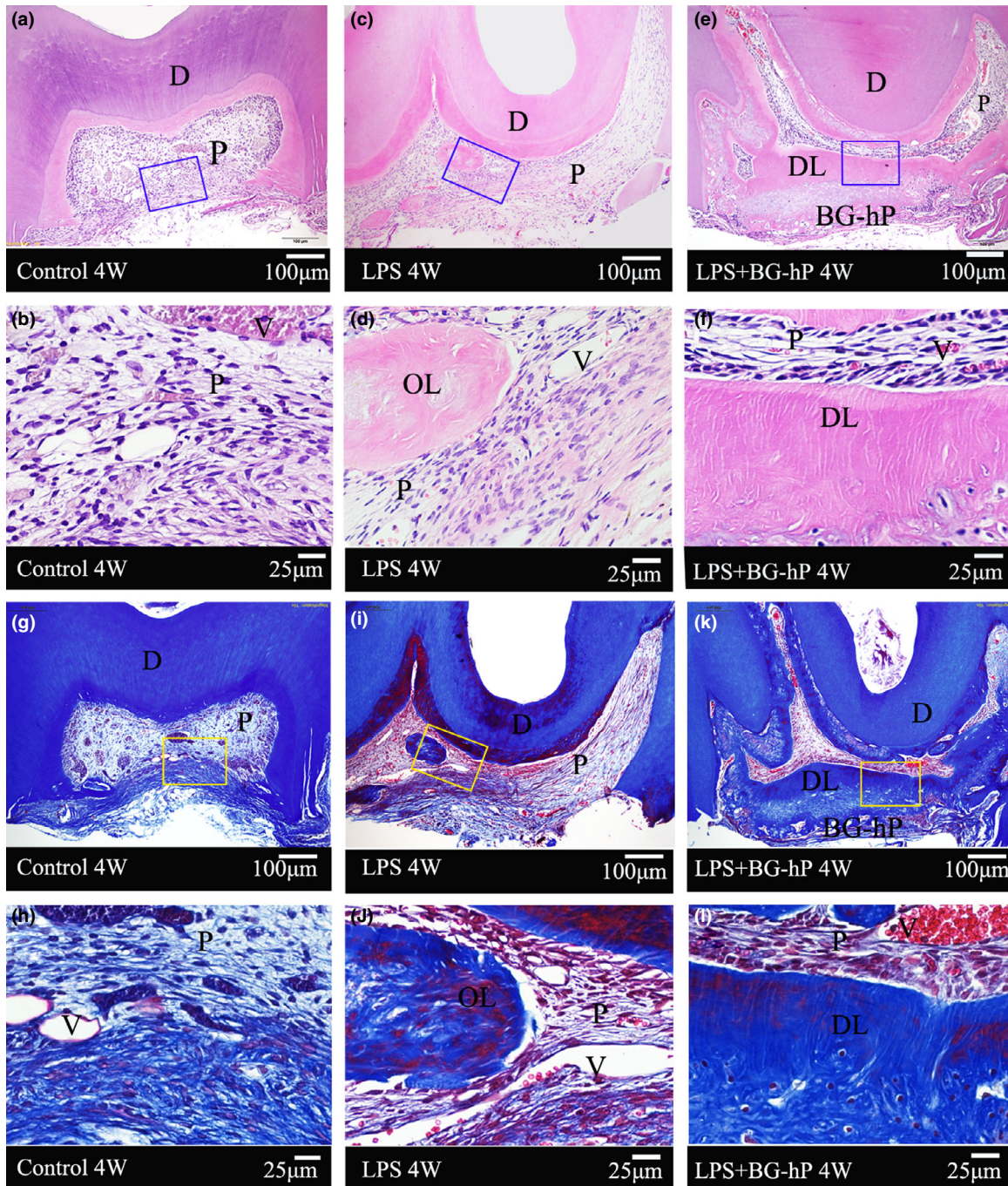


**Figure 4** The effect of BG-hP on the formation of the pulp-dentin complex of pulp tissue stimulated by LPS. HE staining (a–f) and Masson trichrome staining (g–l) of crowns after 4 weeks of subcutaneous transplantation in nude mice *in vivo*. (a, b, g, h): Crowns transplanted alone (b is a magnified image of the blue-boxed areas in a, and h is a magnified image of the yellow boxed areas in g); (c, d, i, j): Crowns pretreated with  $10 \text{ mg mL}^{-1}$  LPS (d is a magnified image of the blue-boxed areas in c, and j is a magnified image of the yellow boxed areas in i); (e, f, k, l): Crowns pretreated with  $10 \text{ mg mL}^{-1}$  LPS and covered with BG-hP (f is a magnified image of the blue-boxed areas in e, and l is a magnified image of the yellow boxed areas in k). Abbreviations: D, dentine; P, pulp tissue; V, blood vessel; DL, dentine-like tissues; OL, osteodentine-like tissue.

and inflammatory cytokines (MacLeod *et al.* 2007). Sodium metasilicate at different concentrations was reported significantly downregulated the production of IL-6 and TNF- $\alpha$  in macrophages after LPS stimulation (Kim *et al.* 2013), which suggested that silicon ions have a crucial anti-inflammatory effect. Calcium silicate-based cements used in endodontics, such as MTA (Dentsply Tulsa), Biodentine (Septodont) or EndoSequence (Brasseler, Savannah, GA, USA), were also reported to decrease the levels of LPS-induced inflammatory mediators (Barbosa *et al.* 2008, Kim *et al.* 2018, Lee *et al.* 2019, Erakovic *et al.* 2020), but some studies reported that ProRoot MTA (Dentsply), Biodentine (Septodont), and Dycal (Dentsply Caulk, Milford, DE, USA) did not have anti-inflammatory effects on LPS-stimulated dental pulp stem cells (Lai *et al.* 2014, Chung *et al.* 2019). In these studies, the co-cultivation methods used for calcium silicate-based cement materials and cells were different, such as direct contact co-cultivation and the use of different concentrations of material-extraction medium for cultivation. Therefore, the effects on the regulation of inflammation may differ based on the difference in composition, ion release and solubility between the materials (Barbosa *et al.* 2008, Lai *et al.* 2014). Furthermore, BG can directly activate genes, such as vascular endothelial growth factor (VEGF) and TGF- $\beta$ 1, which further regulate inflammation (Chen *et al.* 2014). Therefore, BG-hP may inhibit inflammation and regulate the immune response of dental pulp tissues through appropriate ion release, degradation rates and the activation of other cytokines.

Dynamic changes or excess ions may affect cell viability (Alcaide *et al.* 2010, Ajita *et al.* 2015). The rapid release of Ca and/or Na from traditional BGs causes a rapid increase in pH and thus causes cell death, so preconditioning of BG is usually required prior to use (Hirose *et al.* 2016, Ciraldo *et al.* 2018). In this study, although BG-hP inhibited the initial cell number on the first day compared to the control group, cells in the LPS + BG-hP group maintained the same proliferation rate as that in the control group. This result is consistent with the observation that a small increase in Ca concentration was observed only in the first few hours after BG-hP was immersed in SBF, and then, the Ca concentration decreased gradually through binding with P and precipitation over time, thus minimizing the pH change and reducing cell injury (Hoppe *et al.* 2011, Li *et al.* 2017). Even when the BG-hP concentration was increased to 1 mg mL<sup>-1</sup>, the pH remained close to the

physiological optimum (Li *et al.* 2011, Cui *et al.* 2017). Therefore, the superior biocompatibility of this novel high phosphorus containing BG resulted in good cell and tissue responses, even in direct contact with the LPS-stimulated hDPCs.

BG-hP induced odontogenic differentiation and mineralization of the LPS-stimulated hDPCs and promoted the formation of the pulp-dentine complex with homogenous and continuous dentine bridges of the LPS-stimulated pulp, suggesting that the BG-hP promoted LPS-stimulated pulp biomimetic recovery and regeneration. The LPS-stimulated dental pulp tissue formed bone-like mineralization similar to the pathological mineralization of pulp tissue under chronic inflammation stimulation (Goga *et al.* 2008). The calcium-to-phosphorous ratio of the BG-hP that was adopted was 1.62, which is within the optimal range for rapid hydroxyapatite precipitation (Li & Qiu 2011, Li *et al.* 2017). The calcium and silicon ions released by BG promoted odontogenic differentiation and mineralization in hDPCs by activating the MAPK pathway (Rashid *et al.* 2003, Canadillas *et al.* 2010, Liu *et al.* 2014). Silicon ions activate the ERK and p38 pathways and promote the adhesion, proliferation and differentiation of dental pulp cells (Wu *et al.* 2014). Inorganic phosphates are essential for the formation of hydroxyapatite crystals and affect the expression of differentiation-related genes (Beck *et al.* 2003, Mansfield *et al.* 2003). In the near future, the appropriate formulations of the BG-hP to meet the needs of different applications in pulp preservation and regeneration will be explored, and *in vivo* orthotopic models compared with appropriate materials will be used to verify its anti-inflammation and regeneration-inducing abilities.

## CONCLUSIONS

The present preliminary results demonstrated that BG with a high proportion of phosphorus could inhibit the inflammatory response and promote the formation of the pulp-dentine complex in rats. This study will provide a foundation for the construction of materials with dual functions of exerting anti-inflammatory activity and promoting tissue regeneration to meet the needs of dental pulp repair and regeneration.

## Acknowledgements

The authors are grateful for the support of the National Natural Science Foundation of China

(81700953, 51372005, and 81870753). We also thank Professor Dong Qiu (Institute of Chemistry, Chinese Academy of Sciences, Beijing, China) for generously offering the BG materials.

### Conflict of interest

The authors have stated explicitly that there are no conflicts of interest in connection with this article.

### References

- Abou Neel EA, Pickup DM, Valappil SP, Newport, RJ, Knowles, JC (2009) Bioactive functional materials: a perspective on phosphate-based glasses. *Journal of Materials Chemistry* **19**, 690–707.
- Ajita J, Saravanan S, Selvamurugan N (2015) Effect of size of bioactive glass nanoparticles on mesenchymal stem cell proliferation for dental and orthopedic applications. *Materials Science & Engineering* **53**, 142–9.
- Alcaide M, Serrano MC, Roman J *et al.* (2010) Suppression of anoikis by collagen coating of interconnected macroporous nanometric carbonated hydroxyapatite/agarose scaffolds. *Journal of Biomedical Materials Research Part A* **95**, 793–800.
- Ballini, A, Scacco, S, Coletti, D, Pluchino, S, Tatullo, M (2017) Mesenchymal stem cells as promoters, enhancers, and playmakers of the translational regenerative medicine. *Stem Cells International* **2017**, 3292810.
- Ballini, A, Cantore, S, Scacco, S, Coletti, D, Tatullo, M (2018) Mesenchymal stem cells as promoters, enhancers, and playmakers of the translational regenerative medicine 2018. *Stem Cells International* **2018**, 6927401.
- Barbosa SM, Vieira LQ, Sobrinho AP (2008) The effects of mineral trioxide aggregates on cytokine production by mouse pulp tissue. *Oral Surgery, Oral Medicine, Oral Pathology, Oral Radiology, and Endodontics* **105**, e70–e76.
- Barkhordar RA, Hayashi C, Hussain MZ (1999) Detection of interleukin-6 in human dental pulp and periapical lesions. *Endodontics & Dental Traumatology* **15**, 26–7.
- Beck GJ, Moran E, Knecht N (2003) Inorganic phosphate regulates multiple genes during osteoblast differentiation, including Nrf2. *Experimental Cell Research* **288**, 288–300.
- Bindal P, Ramasamy TS, Abu Kasim NH, Gnanasegaran N, Chai WL (2018) Immune responses of human dental pulp stem cells in lipopolysaccharide-induced microenvironment. *Cell Biology International* **42**, 832–40.
- Bogen G, Kim JS, Bakland LK (2008) Direct pulp capping with mineral trioxide aggregate: an observational study. *Journal of the American Dental Association* **139**, 305–15.
- Canadillas S, Canalejo R, Rodriguez-Ortiz ME *et al.* (2010) Upregulation of parathyroid VDR expression by extracellular calcium is mediated by ERK1/2-MAPK signaling pathway. *American Journal of Physiology-Renal Physiology* **F1197–F1204**.
- Cao G, Yang Q, Zhang S *et al.* (2014) Mesenchymal stem cells prevent restraint stress-induced lymphocyte depletion via interleukin-4. *Brain Behavior and Immunity* **38**, 125–32.
- Chen Z, Wu C, Gu W, Klein T, Crawford R, Xiao Y (2014) Osteogenic differentiation of bone marrow MSCs by beta-tricalcium phosphate stimulating macrophages via BMP2 signalling pathway. *Biomaterials* **35**, 1507–18.
- Chung M, Lee S, Chen D *et al.* (2019) Effects of different calcium silicate cements on the inflammatory response and odontogenic differentiation of lipopolysaccharide-stimulated human dental pulp stem cells. *Materials (Basel)* **12**, 1259.
- Ciraldo FE, Boccardi E, Melli V, Westhauser F, Boccaccini AR (2018) Tackling bioactive glass excessive in vitro bioreactivity: preconditioning approaches for cell culture tests. *Acta Biomaterialia* **75**, 3–10.
- Cui C, Wang S, Ren H *et al.* (2017) Regeneration of dental-pulp complex-like tissue using phytic acid derived bioactive glasses. *RSC Advances* **7**, 22063–70.
- Dong X, Chang J, Li H (2017) Bioglass promotes wound healing through modulating the paracrine effects between macrophages and repairing cells. *Journal of Materials Chemistry B* **5**, 5240–50.
- Donnell MDO, Watts SJ, Law RV, Hill RG (2008) Effect of P2O5 content in two series of soda lime phosphosilicate glasses on structure and properties - Part II: physical properties. *Journal of Non-Crystalline Solids* **354**, 3554–60.
- Elsalhy M, Azizieh F, Raghupathy R (2013) Cytokines as diagnostic markers of pulpal inflammation. *International Endodontic Journal* **46**, 573–80.
- Erakovic M, Duka M, Bekic M *et al.* (2020) Anti-inflammatory and immunomodulatory effects of Biodentine on human periapical lesion cells in culture. *International Endodontic Journal* **53**, 1398–412.
- Farges JC, Carrouel F, Keller JF *et al.* (2011) Cytokine production by human odontoblast-like cells upon Toll-like receptor-2 engagement. *Immunobiology* **216**, 513–7.
- Gandolfi MG, Siboni F, Primus CM, Prati C (2014) Ion release, porosity, solubility, and bioactivity of MTA Plus tricalcium silicate. *Journal of Endodontics* **40**, 1632–7.
- Goga R, Chandler NP, Oginni AO (2008) Pulp stones: a review. *International Endodontic Journal* **41**, 457–68.
- Gomez-Cerezo N, Casarrubios L, Morales I *et al.* (2018) Effects of a mesoporous bioactive glass on osteoblasts, osteoclasts and macrophages. *Journal of Colloid and Interface Science* **528**, 309–20.
- Gough JE, Jones JR, Hench LL (2004) Nodule formation and mineralisation of human primary osteoblasts cultured on a porous bioactive glass scaffold. *Biomaterials* **25**, 2039–46.
- Gronthos S, Mankani M, Brahimi J, Robey PG, Shi S (2000) Postnatal human dental pulp stem cells (DPSCs) in vitro and in vivo. *Proceedings of the National Academy of Sciences* **97**, 13625–30.

- Hench LL, Paschall HA (1973) Direct chemical bond of bioactive glass-ceramic materials to bone and muscle. *Journal of Biomedical Materials Research Part A* **7**, 25–42.
- Hirose Y, Yamaguchi M, Kawabata S et al. (2016) Effects of extracellular pH on dental pulp cells in vitro. *Journal of Endodontics* **42**, 735–41.
- Hoppe A, Guldal NS, Boccaccini AR (2011) A review of the biological response to ionic dissolution products from bioactive glasses and glass-ceramics. *Biomaterials* **32**, 2757–74.
- Hossein-Khannazer N, Hashemi SM, Namaki S, Ghanbarian H, Sattari M, Khojasteh A (2019) Study of the immunomodulatory effects of osteogenic differentiated human dental pulp stem cells. *Life Sciences* **216**, 111–8.
- Huang Y, Wu C, Zhang X, Chang J, Dai K (2018) Regulation of immune response by bioactive ions released from silicate bioceramics for bone regeneration. *Acta Biomaterialia* **66**, 81–92.
- Jebahi S, Oudadesse H, Jardak N et al. (2013) Biological therapy of strontium-substituted bioglass for soft tissue wound-healing: responses to oxidative stress in ovariectomized rats. *Annales Pharmaceutiques Francaises* **71**, 234–42.
- Jung JY, Woo SM, Kim WJ et al. (2017) Simvastatin inhibits the expression of inflammatory cytokines and cell adhesion molecules induced by LPS in human dental pulp cells. *International Endodontic Journal* **50**, 377–86.
- Kim DH, Jang JH, Lee BN et al. (2018) Anti-inflammatory and mineralization effects of ProRoot MTA and endocem MTA in studies of human and rat dental pulps in vitro and in vivo. *Journal of Endodontics* **44**, 1534–41.
- Kim EJ, Bu SY, Sung MK, Kang MH, Choi MK (2013) Analysis of antioxidant and anti-inflammatory activity of silicon in murine macrophages. *Biological Trace Element Research* **156**, 329–37.
- Lai WY, Kao CT, Hung CJ, Huang TH, Shie MY (2014) An evaluation of the inflammatory response of lipopolysaccharide-treated primary dental pulp cells with regard to calcium silicate-based cements. *International Journal of Oral Science* **6**, 94–8.
- Lee BN, Hong JU, Kim SM et al. (2019) Anti-inflammatory and osteogenic effects of calcium silicate-based root canal sealers. *Journal of Endodontics* **45**, 73–8.
- Li, Z, Jiang, CM, An, S et al. (2014) Immunomodulatory properties of dental tissue-derived mesenchymal stem cells. *Oral Diseases* **20**, 25–34.
- Li A, Lv Y, Ren H et al. (2017) In vitro evaluation of a novel pH neutral calcium phosphosilicate bioactive glass that does not require preconditioning prior to use. *International Journal of Applied Glass Science* **8**, 403–11.
- Li A, Qiu D (2011) Phytic acid derived bioactive CaO-P2O5-SiO2 gel-glasses. *Journal of Materials Science Materials in Medicine* **22**, 2685–91.
- Li A, Wang D, Xiang J et al. (2011) Insights into new calcium phosphosilicate xerogels using an advanced characterization methodology. *Journal of Non Crystalline Solids* **357**, 3548–55.
- Liu CH, Hung CJ, Huang TH, Lin CC, Kao CT, Shie MY (2014) Odontogenic differentiation of human dental pulp cells by calcium silicate materials stimulating via FGFR/ERK signaling pathway. *Materials Science & Engineering* **43**, 359–66.
- MacLeod RJ, Hayes M, Pacheco I (2007) Wnt5a secretion stimulated by the extracellular calcium-sensing receptor inhibits defective Wnt signaling in colon cancer cells. *American Journal of Physiology-Gastrointestinal and Liver Physiology* **293**, G403–G411.
- Mansfield K, Pucci B, Adams CS, Shapiro IM (2003) Induction of apoptosis in skeletal tissues: phosphate-mediated chick chondrocyte apoptosis is calcium dependent. *Calcified Tissue International* **73**, 161–72.
- Marrazzo P, Paduano F, Palmieri F, Marrelli M, Tatullo M (2016) Highly efficient in vitro reparative behaviour of dental pulp stem cells cultured with standardised platelet lysate supplementation. *Stem Cells International* **2016**, 7230987.
- Martinez FO, Sica A, Mantovani A, Locati M (2008) Macrophage activation and polarization. *Frontiers in Bioscience-Landmark* **13**, 453–61.
- Midha S, Kim TB, van den Bergh W, Lee PD, Jones JR, Mitchell CA (2013) Preconditioned 70S30C bioactive glass foams promote osteogenesis in vivo. *Acta Biomaterialia* **9**, 9169–82.
- Omi M, Hata M, Nakamura N et al. (2016) Transplantation of dental pulp stem cells suppressed inflammation in sciatic nerves by promoting macrophage polarization towards anti-inflammation phenotypes and ameliorated diabetic polyneuropathy. *Journal of Diabetes Investigation* **7**, 485–96.
- Parirokh M, Torabinejad M, Dummer PMH (2018) Mineral trioxide aggregate and other bioactive endodontic cements: an updated overview - part I: vital pulp therapy. *International Endodontic Journal* **51**, 177–205.
- Park HC, Quan H, Zhu T, Kim Y, Kim B, Yang HC (2017) The effects of M1 and M2 macrophages on odontogenic differentiation of human dental pulp cells. *Journal of Endodontics* **43**, 596–601.
- Rashid F, Shiba H, Mizuno N et al. (2003) The effect of extracellular calcium ion on gene expression of bone-related proteins in human pulp cells. *Journal of Endodontics* **29**, 104–7.
- Renard E, Gaudin A, Bienvenu G et al. (2016) Immune cells and molecular networks in experimentally induced pulpitis. *Journal of Dental Research* **95**, 196–205.
- Sadowska JM, Wei F, Guo J et al. (2019) The effect of biomimetic calcium deficient hydroxyapatite and sintered beta-tricalcium phosphate on osteoimmune reaction and osteogenesis. *Acta Biomaterialia* **96**, 605–18.
- Shao M, Wang D, Zhou Y, Du K, Liu W (2020) Interleukin-10 delivered by mesenchymal stem cells attenuates

- experimental autoimmune myocarditis. *International Immunopharmacology* **81**, 106212.
- Silver IA, Deas J, Erecinska M (2001) Interactions of bioactive glasses with osteoblasts in vitro: effects of 45S5 Bioglass, and 58S and 77S bioactive glasses on metabolism, intracellular ion concentrations and cell viability. *Biomaterials* **22**, 175–85.
- Solanki NP, Venkappa KK, Shah NC (2018) Biocompatibility and sealing ability of mineral trioxide aggregate and bio-dentine as root-end filling material: a systematic review. *Journal of Conservative Dentistry* **21**, 10–5.
- Sugiuchi A, Sano Y, Furusawa M, Abe S, Muramatsu T (2018) Human dental pulp cells express cellular markers for inflammation and hard tissue formation in response to bacterial information. *Journal of Endodontics* **44**, 992–6.
- Tokuda M, Nagaoka S, Torii M (2002) Interleukin-10 inhibits expression of interleukin-6 and -8 mRNA in human dental pulp cell cultures via nuclear factor-kappaB deactivation. *Journal of Endodontics* **28**, 177–80.
- Torabinejad M, Parirokh M, Dummer PMH (2018) Mineral trioxide aggregate and other bioactive endodontic cements: an updated overview - part II: other clinical applications and complications. *International Endodontic Journal* **51**, 284–317.
- Wang S, Gao X, Gong W, Zhang Z, Chen X, Dong Y (2014) Odontogenic differentiation and dentin formation of dental pulp cells under nanobioactive glass induction. *Acta Biomaterialia* **10**, 2792–803.
- Wu BC, Kao CT, Huang TH, Hung CJ, Shie MY, Chung HY (2014) Effect of verapamil, a calcium channel blocker, on the odontogenic activity of human dental pulp cells cultured with silicate-based materials. *Journal of Endodontics* **40**, 1105–11.
- Zehnder M, Delaleu N, Du Y, Bickel M (2003) Cytokine gene expression—part of host defence in pulpitis. *Cytokine* **22**, 84–8.
- Zhu N, Chatzistavrou X, Ge L, Qin M, Wang PP, Wang Y (2019) Biological properties of modified bioactive glass on dental pulp cells. *Journal of Dentistry* **83**, 18–26.